

# Implementation of a discrete nodal model to probe the effect of size-dependent surface tension on nanoparticle formation and growth

D. Mukherjee<sup>a, b</sup>, A. Prakash<sup>a, b</sup>, M.R. Zachariah<sup>a, b, \*</sup>

<sup>a</sup>Department of Mechanical Engineering, University of Maryland, College Park, MD, USA

<sup>b</sup>Department of Chemistry and Biochemistry, University of Maryland, College Park, MD, USA

Received 6 August 2005; received in revised form 17 January 2006; accepted 23 January 2006

---

## Abstract

This article presents a study of the effect of size-dependent surface tension, on the formation and evolution of nanoparticles during gas-to-particle conversion. The nuclei formation rates have been computed from chemical reaction like formulation as opposed to the most commonly used expression from kinetic homogeneous nucleation theory derived on the basis of steady-state assumption and capillarity approximation (size-independent constant surface tension). This is achieved with discrete nodal model. We validate the present model by comparing the solution for Aluminum particle growth with our earlier NGDE model [Prakash, A., Bapat, A. P., & Zachariah, M.R. (2003). A simple numerical algorithm and software for solution of nucleation, surface growth, and coagulation problems. *Aerosol Science and Technology*, 37, 892–898], a system that shows a size-dependent surface tension. The results indicate that although the quasi-steady-state assumption of the dynamics is reasonable, the capillarity approximation significantly over-predicts the size of the particles.

© 2006 Published by Elsevier Ltd.

**Keywords:** Size-dependent surface tension; Aerosol GDE; Discrete nodal model; Nucleation kinetics; Surface tension

---

## 1. Introduction

Many materials processing applications occur at elevated temperatures where rapid cooling results in nucleation of metal or refractory from the gas phase. Quenching an aerosol from a thermal plasma reactor for example is a widely known method used for synthesis of ultrafine powder (Girshick & Chiu, 1989). Under these conditions such a system will undergo simultaneous nucleation, coagulation and growth, which may be represented mathematically as species continuity equation for aerosol, generally referred to as the general dynamic equation (GDE). The resulting partial integro-differential equation for the aerosol GDE is analytically intractable, unless the underlying assumptions are strongly relaxed (Gelbard & Seinfeld, 1979; Peterson, Gelbard, & Seinfeld, 1978). Of these, the most relaxed assumptions have been implemented in the derivation for a final expression for the nucleation rate, it being one of the more complex processes.

---

\* Corresponding author. Department of Mechanical Engineering, University of Maryland, College Park, MD, USA. Tel.: +1 301 405 4311; fax: +1 301 314 9477.

E-mail address: [mrz@umd.edu](mailto:mrz@umd.edu) (M.R. Zachariah).

Historically, one of the most common assumptions to solve nucleation as well as evaporation/condensation processes has been that of a constant, size-independent surface tension for the surface energy of nanoparticles (commonly referred to as the capillarity approximation) (Seinfeld & Pandis, 1998). Such an approximation leads to a closed form expression for the nucleation rate that appears in the classical homogeneous nucleation theory. There have been previous efforts to probe the effects of size-dependent surface tension on nucleation theory (Laaksonen & McGraw, 1996; Lu & Jiang, 2004). Laaksonen and McGraw (1996) developed a phenomenological nucleation theory based on the Kelvin relation and Lu and Jiang (2004) had proposed a new model for size-dependent surface energy for nanocrystals. Schmeltzer, Gutzow, and Schmelzer (1996) had also carried out a detailed study of the effect of curvature dependent surface tension on the work of formation of critical clusters in the nucleation theory. While these studies focused on the theoretical aspects involving the analysis of the effect of size-dependent surface tension on nucleation theory, none present a detailed result of its effect on the solution of the aerosol GDE for nanoparticle formation and evolution. The primary goal of the present work is to model the particle formation and evolution processes during gas–particle conversion for a system where the surface tension is known to be size dependent, such that the capillarity approximation is no longer valid.

## 2. Approach

The common assumption of constant surface tension has been a result of historical convenience. Without the ability to know in detail how the surface energy varied with particle size it was a straightforward step to assume it was size invariant. However, the advent of advanced molecular computational tools such as quantum chemistry and molecular dynamics simulation methods has opened the possibility of a more detailed characterization of size effects on surface properties. We have been exploring, using classical molecular dynamics methods, the surface tension of nanoparticles as a function of size. In our prior work we observed that silicon, hydrogenated silicon and silicon oxide (Schweigert, Lehtinen, Carrier, & Zachariah, 2002; Hawa & Zachariah, 2004) has surface tensions that were size invariant. However, more recently we have found that aluminum has a size-dependent surface tension much like prior work on Lennard–Jones particles (Thompson, Gubbins, Walton, Chantry, & Rowlinson, 1984) The implication of that work was that systems for which the chemical bonding climate was angle constrained, as is the case for covalent systems, would not allow the atoms to substantially rearrange themselves as the radius of curvature was increased. In contrast, metals and certainly L–J systems may access a wider range of bonding configurations as the surface is strained and thus the surface normalized energy could change.

The size-dependent surface tension data for aluminum clusters were obtained from our molecular dynamics simulations (Sonwane, Mintmire, & Zachariah, 2005) as shown in Fig. 1 and indicates a monotonically decreasing function with decreasing size. The question for this paper is how does one deal with this in a computationally efficient manner.

The nucleation rate expression shown in Eq. (1) is the subset of the classical nucleation theory and is based only on the assumption of a *quasi-steady-state process*.

$$J = N_1 \left( \sum_{i=1}^{i=\infty} \frac{1}{(k_{f(1,i)}/S) \exp(-\Delta G_i/k_B T)} \right)^{-1}, \quad (1)$$

where,  $N_1$  is the monomer concentration,  $k_{f(1,i)}$  is the forward reaction rate for combination of a monomer and a cluster of size “ $i$ ” based on the free molecular regime collision kernel ( $\text{m}^3\text{s}^{-1}$ ),  $S$  is the saturation ratio,  $k_B$  is the Boltzmann constant (J/K),  $T$  is the temperature in K and  $\Delta G_i$  is the Gibbs’ free energy of formation of an  $i$ -mer.

In principle, Eq. (1) is relatively model independent, as one could supply free energies as a function of cluster size. More commonly the free energy,  $\Delta G_i$  is given by

$$\Delta G_i = k_B T \Theta_i i^{2/3} - i k_B T \ln S. \quad (2)$$

Under the assumption of a capillarity approximation, the non-dimensional surface tension,  $\Theta_i$  of an  $i$ -mer being independent of particle size enables one to determine a critical cluster from the peak of the free energy barrier.

However, it is possible that for size-dependent surface tension the free energy of formation of an  $i$ -mer,  $\Delta G_i$  may not be a simple mono-modal function we have come to expect. Indeed we show by example in Fig. 2, the case of aluminum where the free energy may show a bi-modal distribution depending on the temperature and saturation ratio the system finds itself (e.g. 1500 K,  $S = 1.9$ ). This bi-modal function begs the question: *How do we define a critical cluster size?*

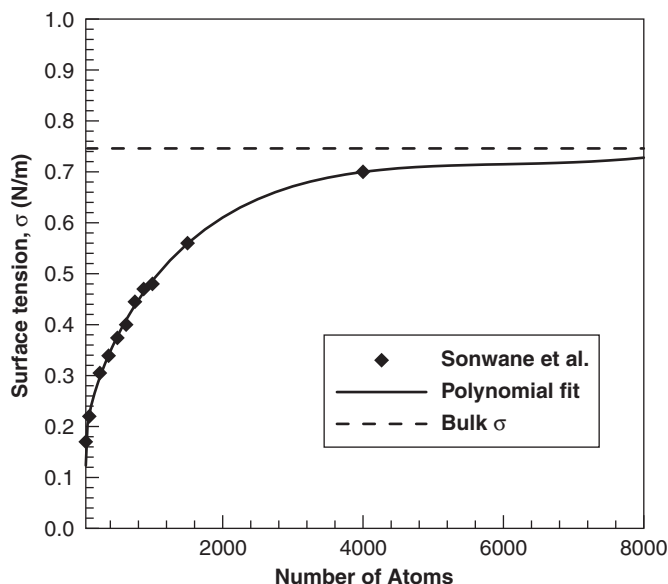


Fig. 1. Variation of surface tension as a function of aluminum cluster size at 1000 K from molecular dynamics simulations.

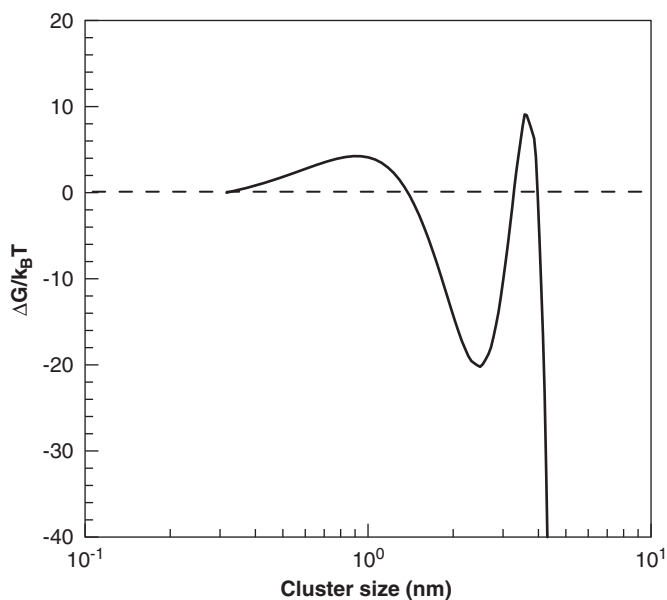


Fig. 2. Free energy of formation of aluminum clusters as a function of cluster size for  $T = 1500$  K and  $S = 1.9$ .

More relevant perhaps is that without a unique defining point to prescribe the critical size one cannot use a unified nucleation rate expression as given by Eq. (1).

Thus, to be able to solve the problem with a size-dependent surface tension the nuclei formation rate must be computed from a model based on reversible chemical reaction processes driven by free energies as opposed to using a single nucleation rate expression. One approach that has been applied is to use the infrastructure of detailed chemical kinetics (Suh, Zachariah, & Girshick, 2001). However, such an approach while quite useful for what is essentially a gas-phase polymerization process is unrealistically complex for a system such as a metal nucleation. Furthermore, such approaches inevitably must make an arbitrary jump between the molecular clusters treated in the formalism of chemical

kinetics and the larger structures treated in the context of aerosol dynamics. For example in our work on silica particle formation (Suh et al., 2001) we truncated the kinetic simulation at a cluster size of (SiO)<sub>10</sub> because of computational tractability and the lack of high quality thermodynamic data. In this paper we will treat the nucleation as a continuum of chemical kinetic processes, which effectively will involve solution of the GDE with variable surface tension.

In the past, several numerical recipes to solve the aerosol GDE have been introduced. Division of particle size domain into sections, commonly known as the sectional method developed by Gelbard, Tambour, and Seinfeld (1980) was the first attempt to solve the GDE numerically. Since then several variants of the sectional method were employed, like the hybrid size grid approach (Jacobson & Turco, 1995), discrete-sectional method (Hounslow, Ryall, & Marshall, 1988; Landgrebe & Pratsinis, 1990; Biswas, Wu, Zachariah, & Mcmillin, 1997) and the nodal method (Lehtinen & Zachariah, 2001). Method of moments (Pratsinis, 1988) is a widely used alternative approach, wherein the size distribution is approximated with a unimodal lognormal function. In an earlier work we presented a relatively inexpensive model (Prakash, Bapat, & Zachariah, 2003) known as NGDE for solving the GDE using a nodal approach. The present paper extends this approach to incorporate a size-dependent surface tension in the solution for nanoparticle evolution processes.

As a case study, as well as to compare our present solution with the earlier NGDE model, we chose to study the evolution of aluminum nanoparticles as an example problem. The results from our present work show that although the steady-state approximation is very reasonable, the elimination of the capillarity approximation implies significant changes in the aerosol evolution, including an over prediction of particle sizes and saturation ratio.

### 3. Numerical model

In the present model, the general dynamic equation (GDE) for nucleation, coagulation and surface growth problem has been mathematically expressed as

$$\frac{dN_k}{dt} = \left. \frac{dN_k}{dt} \right|_{\text{reaction}}^{1 \rightarrow M} + \left. \frac{dN_k}{dt} \right|_{\text{evap/cond}}^{M \rightarrow \text{MAX}} + \left. \frac{dN_k}{dt} \right|_{\text{coag}}^{2 \rightarrow \text{MAX}} \quad (3)$$

Based on our earlier NGDE model (Prakash et al., 2003) we have developed a discrete nodal scheme to solve the aerosol GDE. The present work uses a discrete spacing of nodes at an increment of single monomer for the first *M*-mers, which we refer to as the “nuclei” regime. Thereafter, the nodes have been spaced logarithmically from nodes *M* to *MAX*, which we call the “particle” regime. Fig. 3 illustrates this nodal structure for particle sizes ranging between a monomer and 10 μm. The first *M*-mers were spaced over 30 discrete nodes and the remaining 30 nodes are logarithmically spaced. i.e. *MAX* = 60. The choice of *M* was such that reasonable resolution could be retained to account for the interactions

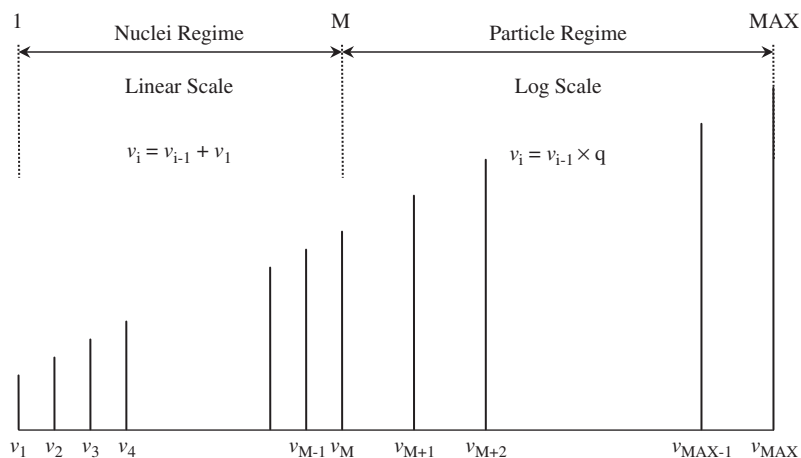


Fig. 3. Schematic of the discrete nodal structure showing the nuclei regime, where the nodes are spaced at an increment of one monomer, and the particle regime where the nodes are spaced on a logarithmic scale.

between monomers and small clusters while keeping the computation time efficient. Choosing MAX as 60 enables us to cover a size range up to 10  $\mu\text{m}$  with approximately 10 nodes per size decade in the particle regime.

In the nuclei regime  $1 \rightarrow M$  cluster growth/decomposition is determined from chemical reaction rates, whereas in the particle regime we have modeled it from heterogeneous condensation/evaporation rates similar to NGDE model (Prakash et al., 2003).

### 3.1. Chemical reaction based nuclei formation

From classical nucleation theory, any cluster growth and decay phenomena is assumed as monomer addition (condensation) or cluster decomposition (evaporation) process analogous to a reversible monomer-cluster “chemical reaction” step given as



where,  $A_k$  represents a cluster of  $k$  molecules ( $k$ -mer). It is noted here that only monomer-cluster interactions are considered in the reaction model whereas all cluster–cluster interactions are accounted for in the coagulation formulation as described later.

In most cases, numerical and analytical solution for nucleation and surface growth part of the GDE incorporates the assumptions of size-independent surface tension for steady-state nucleation processes. Using these approximations, our earlier NGDE is based on the kinetic homogeneous nucleation theory as derived by Girshick and Chiu (1990). In the present work, we solve nucleation without the capillarity approximation using a chemical reaction based formalism. Such a formalism does not require a quasi steady-state assumption. The nucleation rate for any cluster size ( $k$ -mer) is derived from the cluster formation and decomposition rates driven by the corresponding free energy change for a reaction of the form given by Eq. (4). Such an approach implies that the nucleation burst is not confined to a unique critical cluster size, unlike the kinetic homogeneous nucleation theory derived from steady-state assumption. Using this approach, we get the net rate of formation (gas to cluster conversion) of  $k$ -mer in the nuclei regime as

$$\left. \frac{dN_k}{dt} \right|_{\text{reaction}}^{1 \rightarrow M} = N_1 \sum_{k=2}^M \frac{1}{(1 + \delta_{2k})} k_{f(1,k-1)} N_{k-1} - \sum_{k=2}^M k_{b(k)} N_k, \quad (5)$$

where, the first term on the right-hand side accounts for monomer addition (condensation) and the second term represents cluster decomposition (evaporation) process. The Kronecker delta function  $\delta_{2k}$  accounts for the formation of single dimer from the reaction between two monomers. Here the forward reaction rate,  $k_{f(1,k-1)}$  is taken as the free molecular collision kernel between monomer and  $(k-1)$ -mer (see Eq. (11)). The backward reaction rate,  $k_{b(k)}$  for dissociation of a  $k$ -size cluster ( $\text{s}^{-1}$ ) is modeled from the free energy change associated with Eq. (4) and given as (Frankel, 1955):

$$k_{b(k)} = k_{f(1,k-1)} n_s \exp[\Theta_k k^{2/3} - \Theta_{k-1} (k-1)^{2/3}], \quad (6)$$

where  $n_s$  is the equilibrium monomer concentration based on the saturation vapor pressure at temperature  $T$  and  $\Theta_k$  is the non-dimensional surface tension of a  $k$ -mer given as

$$\Theta_k = \frac{s_1 \sigma_k}{k_B T}, \quad (7)$$

where,  $s_1$  is the surface area of a monomer unit ( $\text{m}^2$ ) and  $\sigma_k$  is the surface tension of a particle at the  $k$ th node or a  $k$ -mer ( $\text{N/m}$ ).

Here, the use of size-dependent surface tension,  $\sigma_k$  for any  $k$ -mer negates the assumption of capillarity approximation in the present model. The expression for  $\sigma_k$  was obtained from the polynomial fit to the surface tension for different cluster sizes obtained from our molecular dynamics simulations (Sonwane et al., 2005) at a temperature of 1000 K as shown in Fig. 1. Knowing the bulk surface tension at any temperature, we used the same functional dependence at 1000 K to determine  $\sigma_k$  at that particular temperature.

### 3.2. Evaporation/condensation

In the particle regime ( $M \rightarrow \text{MAX}$ ), particle growth or decay is modeled as condensation, or evaporation of monomers on or, from the surface. The driving force for condensation or evaporation is the difference between the bulk vapor pressure of monomer and the Kelvin effect adjusted vapor pressure over the surface of a particle. In our numerical methodology, the effect of evaporation/condensation on the change in particle size distribution is expressed as

$$\left. \frac{dN_k}{dt} \right|_{\text{evap/cond}} = \begin{cases} \frac{v_1}{v_k - v_{k-1}} k_{f(1,k-1)} (N_1 - N_{1,k-1}^s) N_{k-1} & \text{if } N_1 > N_{1,k-1}^s, \\ -\frac{v_1}{v_{k+1} - v_k} k_{f(1,k+1)} (N_1 - N_{1,k+1}^s) N_{k+1} & \text{if } N_1 < N_{1,k+1}^s, \\ -\frac{v_1}{v_{k+1} - v_k} k_{f(1,k)} (N_1 - N_{1,k}^s) N_k & \text{if } N_1 > N_{1,k}^s, \\ \frac{v_1}{v_k - v_{k-1}} k_{f(1,k)} (N_1 - N_{1,k}^s) N_k & \text{if } N_1 < N_{1,k}^s, \end{cases} \quad (8)$$

where,  $N_{1,k}^s$  is the saturation monomer concentration over the surface of particle at node  $k$  and is derived from Kelvin relation for saturation vapor pressure over a curved surface:

$$N_{1,k}^s = n_s \exp\left(\frac{4\sigma_k v_1}{k_B T d_{p,k}}\right), \quad (9)$$

where,  $v_1$  is the volume of a monomer unit ( $\text{m}^3$ ) and  $d_{p,k}$  is the diameter of a particle at the  $k$ th node. The variation of surface tension,  $\sigma_k$  with particle size has been accounted for in the Kelvin relation when calculating the evaporation/condensation rates at any node  $k$ .

### 3.3. Coagulation

The rate of change of particle size distribution due to coagulation is given by a modified Smoluchowski's equation

$$\left. \frac{dN_k}{dt} \right|_{\text{coag}} \Bigg|_{2 \rightarrow \text{MAX}} = \frac{1}{2} \sum_{\substack{i=2 \\ j=2}} \chi_{ijk} k_{f(i,j)} N_i N_j - N_k \sum_{i=2} k_{f(i,k)} N_i. \quad (10)$$

The first right-hand term is the particle gain at node  $k$  due to collision of two smaller particles, whereas the second term denotes loss of particles from node  $k$  due to collision of particles at node  $k$  with any other particle. Here we have used the collision frequency function  $k_{f(i,j)}$  in the free molecular regime (Friedlander, 2000) defined as

$$k_{f(i,j)} = \left(\frac{3}{4\pi}\right)^{1/6} \left(\frac{6k_B T}{\rho_p}\right)^{1/2} \left(\frac{1}{v_i} + \frac{1}{v_j}\right)^{1/2} (v_i^{1/3} + v_j^{1/3})^2, \quad (11)$$

where,  $\chi_{ijk}$  is the size splitting operator to distribute the particles at the nodes since, in our discrete nodal size space particles exist only at the nodes and  $\rho_p$  is the mass density of particle ( $\text{kg}/\text{m}^3$ ). Particles of volume  $v_i$  and  $v_j$  collide, resulting in a particle of volume  $v_i + v_j$ . If this volume falls between two nodes, the new particle is split into adjacent nodes (Prakash et al., 2003) under the constraint of mass conservation. Thus, we define a size-splitting operator  $\chi_{ijk}$ , as follows:

$$\chi_{ijk} = \begin{cases} \frac{v_{k+1} - (v_i + v_j)}{v_{k+1} - v_k} & \text{if } v_k \leq v_i + v_j \leq v_{k+1}, \\ \frac{(v_i + v_j) - v_{k-1}}{v_k - v_{k-1}} & \text{if } v_{k-1} \leq v_i + v_j \leq v_k, \\ 0, & \text{otherwise.} \end{cases} \quad (12)$$

For transition regime cases, the present model has provisions in the code for the user to opt for Fuchs expression for the collision kernel.

### 3.4. Monomer balance

The gain or loss of monomers due to reaction in the first  $M$  nodes and evaporation/condensation in nodes  $M$  to MAX needs to be accounted for. The monomer population balance can be written as

$$\frac{dN_1}{dt} = \left. \frac{dN_1}{dt} \right|_{\text{reaction}}^{1 \rightarrow M} + \left. \frac{dN_1}{dt} \right|_{\text{evap/cond}}^{M \rightarrow \text{MAX}}, \quad (13)$$

where

$$\left. \frac{dN_1}{dt} \right|_{\text{reaction}}^{1 \rightarrow M} = -N_1 \sum_{k=2}^M k_f N_1 N_{k-1} + \sum_{k=2}^M (1 + \delta_{2k}) k_b N_k \quad (14)$$

and

$$\left. \frac{dN_1}{dt} \right|_{\text{evap/cond}}^{M \rightarrow \text{MAX}} = \begin{cases} -k_{f(1,k-1)}(N_1 - N_{1,k-1}^s)N_{k-1} & \text{if } N_1 > N_{1,k-1}^s, \\ -k_{f(1,k+1)}(N_1 - N_{1,k+1}^s)N_{k+1} & \text{if } N_1 < N_{1,k+1}^s, \\ -k_{f(1,k)}(N_1 - N_{1,k}^s)N_k & \text{if } N_1 > N_{1,k}^s, \\ -k_{f(1,k)}(N_1 - N_{1,k}^s)N_k & \text{if } N_1 < N_{1,k}^s. \end{cases} \quad (15)$$

The Kronecker delta function  $\delta_{2k}$  accounts for the formation of two monomer units due to dissociation of a dimer (since  $\delta_{ij} = 1$ , if  $i = j$ ; otherwise,  $\delta_{ij} = 0$ ).

## 4. Results and discussion

The problem conditions for both algorithm validation and the study of the effect of capillarity approximation were adapted from an earlier work by Panda and Pratsinis (1995). We have modeled the evaporation–condensation of aluminum where aluminum vapor at 1773 K is quenched at a constant cooling rate of 1000 K/s in an aerosol flow reactor.

### 4.1. Algorithm validation

In this section we validate our discrete nodal model by comparing its solution under the assumption of capillarity approximation with that from NGDE for the same problem as described above. The comparisons for the temporal variation of saturation ratio and the particle size distribution, are shown in Figs. 4 and 5, respectively, indicate good agreement between the NGDE and the present model. Figs. 4 and 5 clearly show that steady-state assumption in the NGDE model is a very reasonable approximation. The reaction rates in the nuclei regime are very fast as compared to the overall aerosol kinetics, thereby leading the system quickly to a quasi equilibrium state.

### 4.2. Effect of variable surface tension

Finally we turn our attention to the main topic of this paper the role of variable surface tension. We would like to illustrate the assumption of capillarity approximation, by comparing the solution to the GDE for constant and size-dependent surface tension. The aerosol parameters considered for the comparison are saturation ratio, mean diameter, monomer concentration, particle number concentration and particle size distribution.

Fig. 6 shows the temporal variation of saturation ratio ( $S$ ) for the two cases. As seen in the figure,  $S$  peaks with a much lower value at an earlier time when the effects of size-dependent surface tension (variable  $\sigma$ ) are included. Eq. (6) indicates that the backward reaction rate has an exponential dependence on  $\sigma$ . In the case of size-dependent surface tension problem, as the surface tension ( $\sigma$ ) for smaller clusters become significantly smaller than the bulk

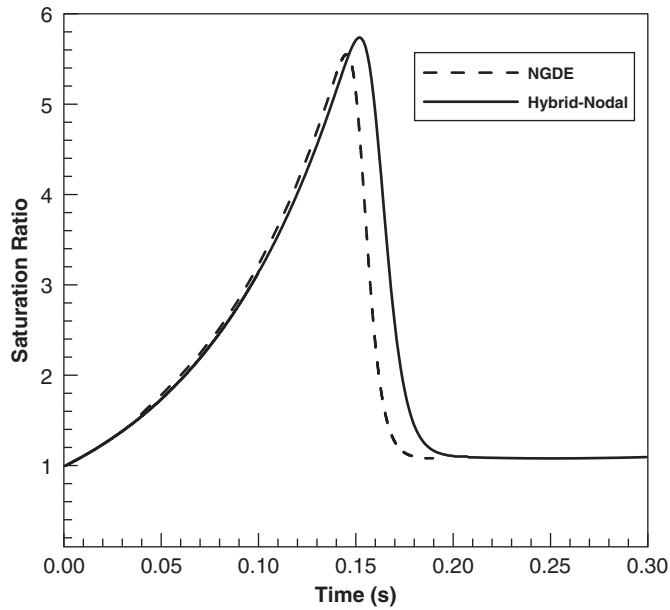


Fig. 4. Temporal evolution of saturation ratio as obtained from NGDE, which assumes steady-state approximation and is based on kinetic homogeneous nucleation theory, and from the discrete nodal method, both solved for the case of constant surface tension.

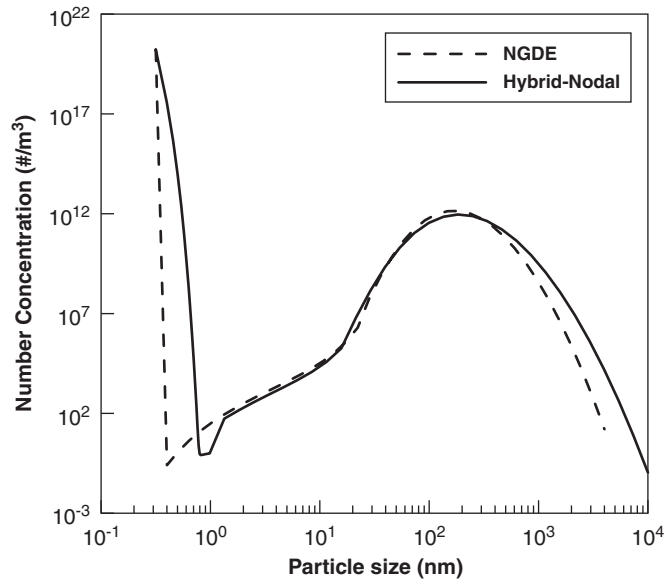


Fig. 5. A comparison of particle size distribution obtained from NGDE and from discrete nodal method for constant surface tension after 0.2 s.

value (Fig. 1), the backward rate constants (evaporation)  $k_{b(k)}$  are greatly suppressed. On the other hand, the forward reaction constant  $k_f$  does not depend on surface tension. This results in an enhanced gas–particle conversion rate and a corresponding faster depletion of monomers. In other words, unlike the constant surface tension case, the evaporation event is much slower in the case of variable surface tension, thereby leading to slower replenishment of monomers and a much smaller supersaturation. This is also supported by the variation of monomer concentrations with time for the two cases shown in Fig. 7. The step like monomer concentration curve for the case of constant surface tension indicates an

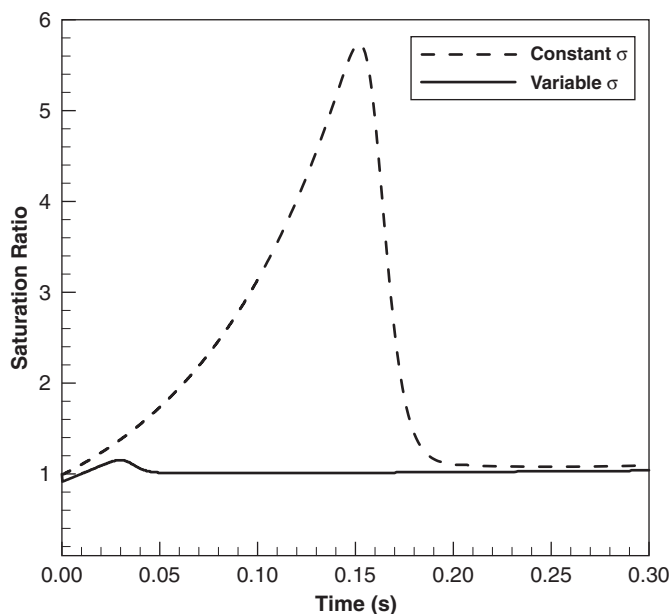


Fig. 6. Comparison of saturation ratio as a function of time for bulk surface tension (constant) and for size-dependent surface tension.

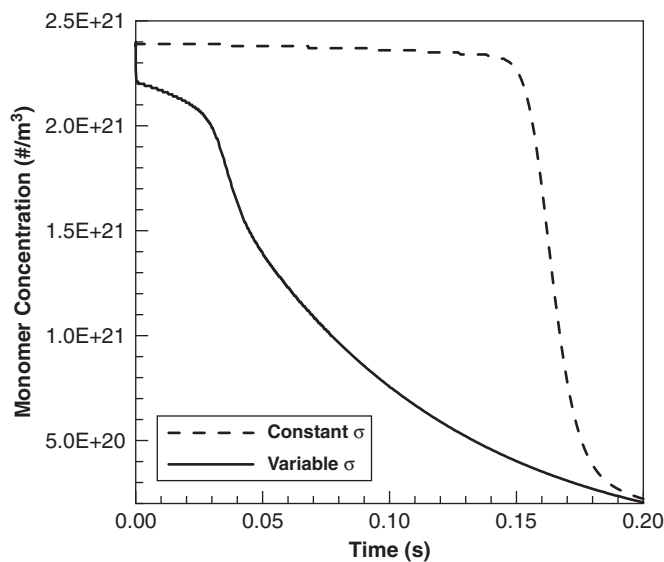


Fig. 7. Comparison of monomer concentration for the solution of general dynamic equation with and without capillarity approximation.

instantaneous nucleation outburst with a sharp drop in the monomer concentration. In contrast, for the case of variable surface tension the drop in monomer concentration is gradual and begins sooner. While the discrete nodal model does not choose a critical cluster size as in classical nucleation theory, the step-like drop in monomer concentration in the case of constant surface tension (Fig. 7) indicates a similar concept of a critical cluster size.

The net effect of this earlier drop in the saturation ratio and monomer concentration is that particle formation occurs sooner as shown in the evolution of the mean particle diameter presented in Fig. 8. While the size-dependent surface tension also plays a role in the evaporation/condensation rates in the particle regime, the effect of variable  $\sigma$  is negligible for particle sizes over 5 nm, where the surface tension asymptotically approaches the bulk value. Since variable surface

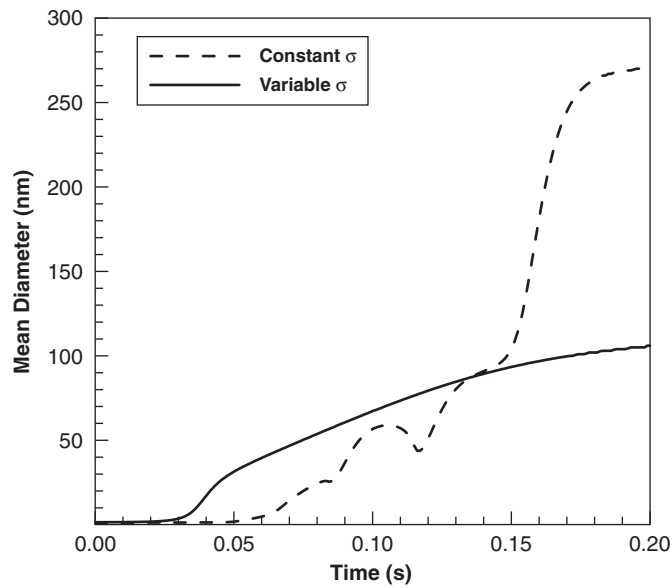


Fig. 8. A size-dependent surface tension results in a smaller average particle size due to slower growth rate (gradient of the curve) compared to the constant surface tension case where the monomer concentration is comparatively high resulting in a faster growth.

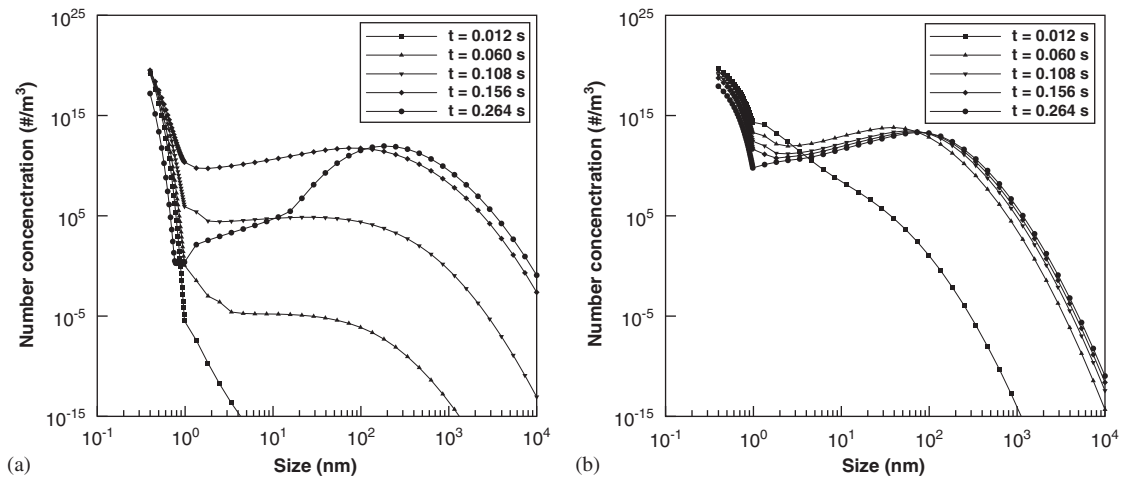


Fig. 9. Temporal evolution of particle size distribution for the two cases under study: (a) for constant surface tension; (b) for variable surface tension show that size-dependent surface tension results in a larger number concentration of particles in the smaller size range and a smaller number concentration in the large size range.

tension should enhance net particle formation due to the lower evaporation rate of clusters we see, from the comparison of temporal evolution of particle size distribution for variable and constant surface tension in Fig. 9a,b, that in the case of variable surface tension larger particle sizes attain higher number concentration earlier in time as compared to the constant surface tension case. Also, unlike the constant surface tension case, the final particle size distribution for variable surface tension at  $t = 0.264$  s indicate a relatively large number concentration in the particle size range of 1 – 100 nm as shown in Fig. 9a,b.

The combined effect of a large number of smaller clusters and a lower monomer concentration retards the surface growth of particles in the case of variable surface tension. This suppressed growth process is evident in Fig. 8 from the gradual rise in mean particle diameter beyond 0.15 s in the case of variable  $\sigma$  whereas its counter part constant  $\sigma$

case exhibits a much enhanced growth rate (steeper gradient of mean diameter) resulting in a larger mean diameter. The predominant growth mechanism in the constant  $\sigma$  case is the monomer–particle interaction ( $A_1 + A_g \leftrightarrow A_{g+1}$ ) whereas the cluster–particle interaction ( $A_k + A_g \leftrightarrow A_{k+g}$ , where  $k$  is a small cluster) dominates the growth process in the case of variable  $\sigma$ . The steep growth in constant  $\sigma$  case is a result of a large number concentration of monomers ( $\sim 0.15$  s in Fig. 7) coupled with the fast monomer–particle collision kernel. In contrast, a lower monomer concentration and a smaller collision kernel for cluster–particle interaction results in a slower particle growth.

## 5. Conclusions

In this article, we have developed a discrete nodal model based on our earlier NGDE model to study the effect of size-dependent surface tension on the evolution of nanoparticle grown from gas–particle conversion. The present model couples a chemical reaction based Gibbs’ free energy driven nuclei formation regime (to negate the steady-state and capillarity approximations) with the condensation/evaporation driven particle formation regime similar to the NGDE model. The new model is solved for the growth of aluminum nanoparticles by using a size-dependent surface tension data obtained from earlier molecular dynamics simulations. Although the surface tension of particles larger than 5 nm approaches the bulk value, the final mean diameter predicted using a variable  $\sigma$  ( $\sim 270$  nm) is significantly smaller compared to that predicted using a constant  $\sigma$  ( $\sim 100$  nm). This difference is associated with the exponential dependence of backward reaction rate (in the nuclei regime  $< \sim 1$  nm) as manifested through the size-dependent surface tension. Using a variable  $\sigma$  enhances the formation of smaller nuclei (due to reduced backward reaction rate) which then act as sites for heterogeneous growth resulting in a smaller mean particle size. In the case of size-dependent surface tension, a significant difference in the aerosol dynamics was that the particle growth was dominated by cluster–particle interactions rather than the usual monomer–particle interactions for constant surface tension case.

## Acknowledgment

Partial support of this work was provided by the ARMY-DURINT Center for NanoEnergetics Research.

## References

- Biswas, P., Wu, C. Y., Zachariah, M. R., & Mcmillin, B. (1997). Characterization of iron oxide-silica nanocomposites in flames. Part. II. Comparison of discrete-sectional model predictions to experimental data. *Journal of Materials Research*, 12(3), 714–723.
- Frankel, J. (1955). *Kinetic theory of liquids*. New York: Dover.
- Friedlander, S. K. (2000). *Smoke dust and haze*. Oxford: Oxford University Press, p. 210.
- Gelbard, F., & Seinfeld, J. H. (1979). The general dynamics equation for aerosols. *Journal of Colloid and Interface Science*, 68(2), 363–382.
- Gelbard, F., Tambour, Y., & Seinfeld, J. H. (1980). Sectional representations for simulating aerosol dynamics. *Journal of Colloid and Interface Science*, 76(2), 541–556.
- Girshick, S. L., & Chiu, C. P. (1989). Homogeneous nucleation of particles from the vapor phase in thermal plasma synthesis. *Plasma Chemistry and Plasma Processing*, 9(3), 355–369.
- Girshick, S. L., & Chiu, C. P. (1990). Kinetic nucleation theory: A new expression for the rate of homogeneous nucleation from an ideal supersaturated vapor. *Journal of Chemical Physics*, 93, 1273–1277.
- Hawa, T., & Zachariah, M. R. (2004). Internal pressure and surface tension of bare and hydrogen coated silicon nanoparticles. *Journal of Chemical Physics*, 121(18), 9043–9049.
- Hounslow, M. J., Ryall, R. L., & Marshall, V. R. (1988). A discretized population balance for nucleation, growth and aggregation. *AIChE Journal*, 34(11), 1821–1832.
- Jacobson, M. Z., & Turco, R. P. (1995). Simulating condensational growth, evaporation, and coagulation of aerosols using a combined moving and stationary size grid. *Aerosol Science and Technology*, 22, 73–92.
- Laaksonen, A., & McGraw, R. (1996). Thermodynamics, gas–liquid nucleation and size-dependent surface tension. *Europhysics Letters*, 35, 367–372.
- Landgrebe, J. D., & Pratsinis, S. E. (1990). A discrete-sectional model for particulate production by gas-phase chemical reaction and aerosol coagulation in the free-molecular regime. *Journal of Colloid and Interface Science*, 139(1), 63–86.
- Lehtinen, K. E. J., & Zachariah, M. R. (2001). Self-preserving theory for the volume distribution of particles undergoing brownian coagulation. *Journal of Colloid and Interface Science*, 242, 314–318.
- Lu, H. M., & Jiang, Q. (2004). Size-dependent surface energies of nanocrystals. *Journal of Physical Chemistry B*, 108, 5617–5619.

- Panda, S., & Pratsinis, S. E. (1995). Modeling the synthesis of aluminum particles by evaporation–condensation in an aerosol flow reactor. *NanoStructured Materials*, 5, 755–767.
- Peterson, T. W., Gelbard, F., & Seinfeld, J. H. (1978). Dynamics of source-reinforced, coagulating, and condensing aerosols. *Journal of Colloid and Interface Science*, 63, 426–445.
- Prakash, A., Bapat, A. P., & Zachariah, M. R. (2003). A simple numerical algorithm and software for solution of nucleation, surface growth, and coagulation problems. *Aerosol Science and Technology*, 37, 892–898.
- Pratsinis, S. E. (1988). Simultaneous nucleation, condensation, and coagulation in aerosol reactors. *Journal of Colloid and Interface Science*, 124(2), 416–427.
- Schmeltzer, J. W. P., Gutzow, I., & Scmelzer, J. Jr. (1996). Curvature-dependent surface tension and nucleation theory. *Journal of Colloid and Interface Science*, 78, 657–665.
- Schweigert, I. V., Lehtinen, K. E. J., Carrier, M. J., & Zachariah, M. R. (2002). Structure and properties of silica nanoclusters at high temperatures. *Physics Review B*, 5(23), 235410/1–235410/9.
- Seinfeld, J. H., & Pandis, S. N. (1998). *Atmospheric chemistry and physics*. New York: Wiley.
- Sonwane, C. G., Mintmire, J., & Zachariah, M. R., 2005. Structure and interfacial properties of bare and oxide coated aluminum nanoclusters, submitted for publication.
- Suh, S. M., Zachariah, M. R., & Girshick, S. L. (2001). Modeling particle formation during low pressure silane oxidation: Detailed chemical kinetics and aerosol dynamics. *Journal of Vacuum Science and Technology A*, 19, 940–951.
- Thompson, S. M., Gubbins, K. E., Walton, J. P. R. B., Chantry, R. A. R., & Rowlinson, J. S. (1984). A molecular dynamics study of liquid drops. *Journal of Chemical Physics*, 81, 530–542.